Journal of Applied Polymer Science

Rheological Behavior - Electrical and Thermal Properties of Polypyrrole/Graphene Oxide Nanocomposites

P. Manivel,[1] S. Kanagaraj,[2] A. Balamurugan,[1] N. Ponpandian,[1] D. Mangalaraj,[1] C. Viswanathan[1]

[1]Department of Nanoscience and Technology, Bharathiar University, Coimbatore 641 046, Tamil Nadu, India
[2]Department of Mechanical Engineering, Indian Institute of Technology, Guwahati 781 039, Assam, India
Correspondence to: C. Viswanathan (E-mail: viswanathan@buc.edu.in)

ABSTRACT: Polypyrrole/graphene oxide (Ppy/GO) nanocomposites were synthesized via *in situ* polymerization of pyrrole in the presence of GO at various proportions (1–5%). They were characterized to determine their electrical, thermal, and rheological properties by various techniques. The aim of this study was to determine the rheological behavior of Ppy/GO nanocomposite at different mass ratios (100 : 1, 100 : 2, 100 : 3, 100 : 4, and 100 : 5%) and temperature (25–180°C) using a rotational mode in cone-plate method. The shear stress (τ Pa) and viscosity (η Pa s) values of the nanocomposites increased with the increase in GO mass ratio added to Ppy, which was accompanied by an increased flexibility of the nanocomposites due to the higher aspect ratio of the GO sheet. Hence, it is suggested that the GO sheets are effective for the reinforcement of Ppy thereby significantly improvising its thermal stability, electrical conductivity, and rheological properties. © 2014 Wiley Periodicals, Inc. J. Appl. Polym. Sci. **2014**, *131*, 40642.

KEYWORDS: composites; conducting polymers; rheology; thermal properties

Received 21 August 2013; accepted 23 February 2014
DOI: 10.1002/app.40642

INTRODUCTION

Polymer nanocomposite has gained importance in nanoscience and technology offering significant potential in the development of advanced materials in diverse areas such as electronic devices, super capacitors, batteries, sensors, and many other fields.[1,2] The development of polymer nanocomposite with appropriate micro- and nano-structure and with favorable electrical, thermal, and mechanical properties for several technological and medical applications still poses a challenge.[3]

In recent years, extensive research has been done in conducting polymers due to their wide range of applications and also for their interesting chemical and physical properties.[4] Conductive polymers, especially heteroaromatic polypyrrole (Ppy), is considered as one of the most promising material because of its high electrical conductivity, easy preparation, and environmental stability. The characters of Ppy are attributable to its unique π-stacked co-planar structure assisted by π-π conjugation, and become a popular material for advance applications.[5] However, conducting polymers usually show a poor thermal, mechanical, oxidative stability, and insolubility in common solvents and infusibility that limits their commercial application.[6] In order to overcome these problems, several processing methods have been adopted and the product with improved overall properties has been achieved by reinforcing the polymer with different inorganic materials (carbon nanomaterials). The examples of such enhancements in properties include the conducting nanocomposites made by incorporating conductive polymers in inorganic solids such as graphite oxide (GO), montmorillonite, and carbon nanotubes.[7–9]

Graphene, a newly discovered two-dimensional carbon nanomaterial with a one atom thick structure, has received extensive attention due to its unique properties and has emerged as highly promising material for various applications.[10–13] Recently, the oxidative GO, having oxygen as a functional group on its basal plane and edges, has become a popular matrix material due to its superior structure, mechanical, and thermal properties compared with other conventional incorporating materials.[14–17] GO is an ideal candidate for the synthesis of composite materials and characterized to be a lamellar solid with unoxidized aromatic and aliphatic regions containing hydroxyl, carboxyl and epoxide groups induced by oxidation.[15,18–22]

The nanocomposites comprising of conducting polymers and layered GO often exhibit improved overall properties which are due to the synergic interactions that occur between components.[23] Several GO-based polymer nanocomposites have been developed with marked improvement in thermal, mechanical, and electrical properties.[24,25] Han and Lu synthesized 1,5-naphthalene disulfonic acids doped Ppy/GO nanocomposite

by *in situ* polymerization method[5] and Bissesur et al. reported the insertion of Ppy into layered GO by using the exfoliation and restacking properties.[26] Therefore, numerous studies have been performed to augment the thermal, the electrical, and the mechanical properties of nanocomposites using various inorganic hosts but to the best of our knowledge there are no reports on the effect of GO incorporation on the rheological properties of Ppy.

In this study, we have synthesized Ppy/GO nanocomposite by *in situ* polymerization. GO can be delaminated into nanosheets and homogeneously dispersed in aqueous solution. This work aims at obtaining a good dispersion of GO sheet within the polymer matrix as well as achieving good improvements in thermal and electrical properties. The rheological behavior of the nanocomposites was investigated in terms of their shear viscosity and shear stress. Furthermore, the shear stress and viscosity of the nanocomposites increased with the increase in mass ratios of GO incorporated into Ppy. The introduction of less amount of GO into Ppy was found to greatly enhance the properties of Ppy.

EXPERIMENTAL

Materials

Natural graphite flakes (10 mesh) were purchased from Alfa Aesar. Pyrrole was purchased from Himedia chemical and was distilled under reduced pressure and kept below 0°C before use. Sodium nitrates, sulfuric acid, hydrochloric acid, potassium permanganate, and ammonium peroxydisulfate were obtained from Himedia chemicals and hydrogen peroxide was from Sd-fine chemicals. All the analytical-reagent grade chemicals were used without further purification. All the aqueous solutions were prepared with double-distilled water.

Synthesis of Polypyrrole Nanoparticles

Pyrrole was first distilled under vacuum to remove the oxidative impurities. The purified pyrrole (0.2*M*) was dissolved in 100 mL of 1*M* HCl aqueous solution. While maintaining vigorous stirring, the ammonium peroxydisulfate (0.25*M*) aqueous solution (ammonium peroxydisulfate in 50 mL of 1*M* HCl) was slowly added drop wise into the pyrrole solution. Polymerization was observed after complete addition of ammonium peroxydisulfate and the characteristic black color of Ppy emeraldine salt appeared. The mixture was stirred overnight at 0–5°C. The precipitated Ppy was collected by filtration and repetitively washed with double distilled water, ethanol, and acetone successively until the filtrate became colorless and was dried in vacuum oven at 60°C overnight.

Synthesis of Polypyrrole/Graphene Oxide Nanocomposites

Ppy/GO was prepared by *in situ* polymerization of pyrrole in a suspension of GO in acidic solution. GO was synthesized from natural graphite flakes by a modified Hummers method.[27] The weight ratio of pyrrole to GO was varied as 100 : 1, 100 : 2, 100 : 3, 100 : 4, and 100 : 5 and the resulting composites were named as Ppy/GO1, Ppy/GO2, Ppy/GO3, Ppy/GO4, and Ppy/GO5, respectively. Typically, the GO was dispersed in 100 mL of 1*M* HCl aqueous solution by bath sonicating for 1 h. Then, 0.2*M* pyrrole was dissolved in the GO containing acidic aqueous solution. While maintaining vigorous stirring at room temperature, ammonium peroxydisulfate solution, with a mole ratio to aniline of 1 : 2, in 1*M* HCl was added drop wise into the resulting mixture. After about 5 min of addition, the pyrrole started to polymerize while the color of mixture changed into black. The mixture was stirred at 0–5°C overnight. The composites were collected by filtration and repetitively washed with double distilled water, ethanol, and acetone successively until the filtrate became colorless and dried in vacuum oven at 60°C overnight.

Characterization

The Fourier transform infrared (FTIR) spectra of the samples were recorded on a Thermonicolet 10—ATR mode FTIR spectrometer by using KBr pellets to confirm the presence of functional groups. X-ray diffraction (XRD) patterns were recorded on an X-pert Pro' PANlytical powder X-ray diffractometer. Copper Kα line was used as the radiation source with $\lambda = 1.5406$ Å. Raman spectra were recorded at ambient temperature on a Horiba Jobin-LabRam-HR UV spectrometer with Argon laser at an excitation wavelength of 514 nm. QUANTA FEG-250 field emission scanning electron microscope (FE-SEM) was used to determine the morphology of the composites. TGA was performed using a SEIKO-TG/DTA 6200 instrument in the temperature range of 23–800°C with a heating rate of 20°C/min under constant nitrogen flow to study the thermal degradation of the samples. The electrical conductivity measurement was studied by impedance measurement using a computer controlled impedance analyzer HIOKI 3532 LCR HITESTER in the frequency ranging from 50 Hz to 10 kHz. The powder was pressed into a 3 mm diameter pellet under identical conditions. The pellet was then dried in vacuum for 1 h before measurement.

Rheological Measurements

The synthesized Ppy/GO nanocomposite particles were stored in vacuum desiccators prior to use. The rheological fluid was prepared by dispersing 100 mg of Ppy/GO nanocomposite particles in 2 mL silicone oil with the help of an ultrasonicator for better dispersion. The rheological measurements of the nanocomposite were taken in an Anton paar rheometer (Physica MCR 101). The shear stress/shear rate and shear viscosity/shear rate rotation ramp tests were performed using a cone sensor (CP50-1-SN22160; 50 mm diameter, 1° angle), with 0.099 mm gap. The samples were measured at different temperatures (25, 100, 150, 180°C). The flow curves of shear stress versus shear rate were carried out in the range of 1–1000 s^{-1}. The sample was not reused after heating due to the change in rheological properties.

RESULTS AND DISCUSSIONS

Characteristics of Polypyrrole/Graphene Oxide Nanocomposite

In *in situ* chemical polymerization of Ppy/GO nanocomposite, it was important to take into consideration, the electron transport properties of both GO and pyrrole monomer in order to determine the molecular binding mechanism as shown in Figure 1. The functional groups —OH, —COOH, and epoxy exist on the surface and pores of the GO sheet were dispersed by ultrasonication. When pyrrole was added into the brown suspension, it gets adsorbed onto the electronegative oxygen atoms of GO sheets and all pyrrole monomer begin to polymerize.

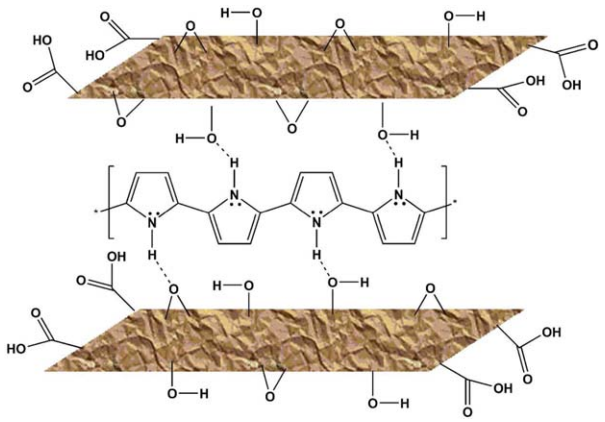

Figure 1. Schematic representation depicting interaction of GO sheet and Ppy chain. [Color figure can be viewed in the online issue, which is available at wileyonlinelibrary.com.]

The resulting nanocomposite structure was GO sheets coated by Ppy and the Ppy insertion between the GO sheets was by hydrogen bonding of GO to the Ppy backbone.

Figure 2 displays the FTIR spectra of oxidized GO, Ppy, and Ppy/GO nanocomposites. GO sheet showed the characteristic peaks at 1050, 1242, 1384, 1630, and 1732 cm^{-1} that corresponds to the C—O—C stretching vibrations, C—OH stretching peak, O—H deformation of the C—OH group, C=C stretching mode, and C=O stretching vibrations of the —COOH group, respectively. The broad and intense peak corresponding to the

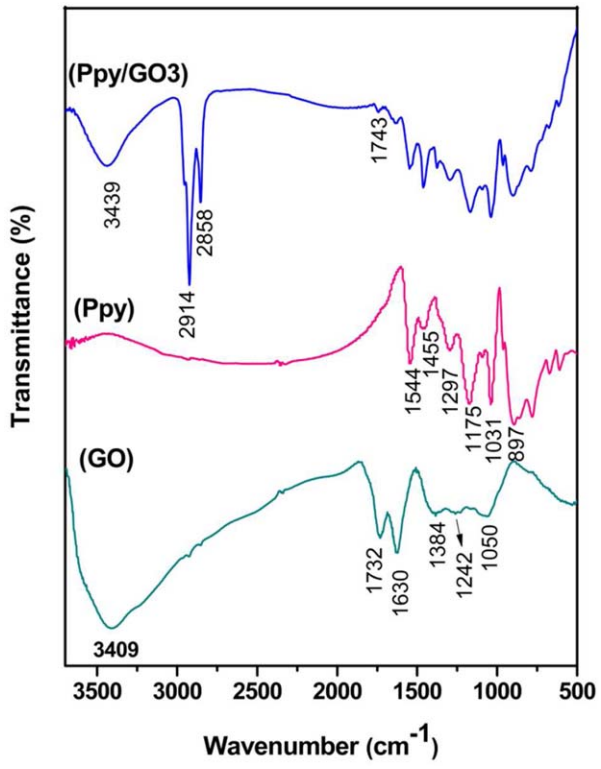

Figure 2. FTIR spectra for GO, Ppy, and Ppy/GO3 nanocomposite. [Color figure can be viewed in the online issue, which is available at wileyonlinelibrary.com.]

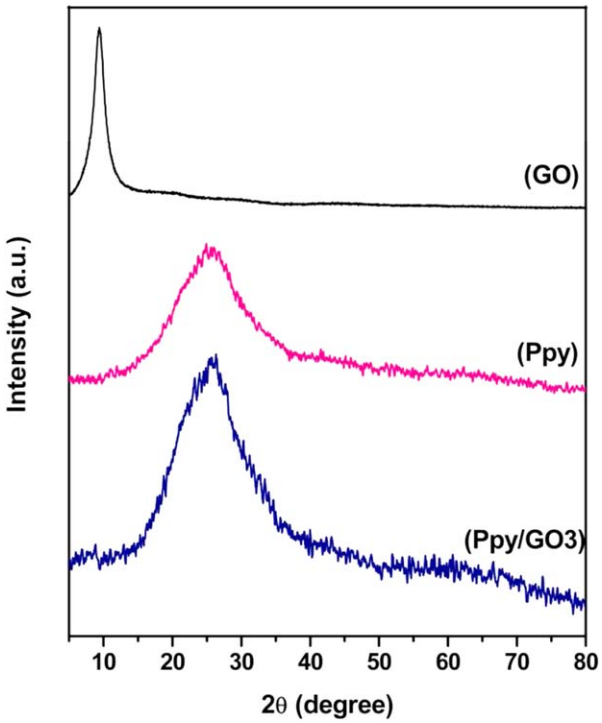

Figure 3. XRD pattern for GO, Ppy, and Ppy/GO3 nanocomposite. [Color figure can be viewed in the online issue, which is available at wileyonlinelibrary.com.]

stretching vibrations of O—H at 3409 cm^{-1} indicated that the GO samples contain large quantity of adsorbed water molecules. These features suggested that GO is heavily oxidized and consists of mainly —OH and other oxygen containing functional groups. In the spectra of Ppy, the strong absorption bands at1544 cm^{-1} and 1455 cm^{-1} corresponds to the C—C stretching vibration in pyrrole ring. The band at 1297 cm^{-1} was due to the C—N in-plane vibration, and the bands at 1175 and 1031 cm^{-1} corresponds to the C—H bending modes while the band at 897 cm^{-1} corresponds to C—H out-of-plane deformation vibration. The FTIR spectrum of Ppy/GO3 nanocomposite was almost the same as that of Ppy. The absorption peaks at 1544, 1455, and 3439 cm^{-1} were associated with the C=C, C—N, and N—H stretching vibration in the Ppy ring. The absorption peaks at 2914 and 2858 cm^{-1} were observed and were ascribed to asymmetric stretching and symmetric vibration of CH_2.[28] It should be noted that the peak due to the C=O group within the Ppy/GO nanocomposite had been shifted to 1743 cm^{-1}, which was probably due to the π-π interaction and hydrogen bonding between the GO sheet and aromatic Ppy rings. The peak at 1640 cm^{-1} indicated the C=C backbone stretching. The characteristic peak of Ppy was seen at 1544 cm^{-1} and 1455 cm^{-1} in the Ppy/GO nanocomposite.[30]

The structure of the composites was investigated by XRD measurements. The XRD patterns of pristine GO, Ppy, and Ppy/GO nanocomposites are shown in Figure 3. The X-ray patterns of GO display the presence of a strong peak at 12° that corresponds to (002) plane which indicate the presence of residual stacked layer of GO with functional group oxygen, which was formed during oxidation. According to Bragg's law, the

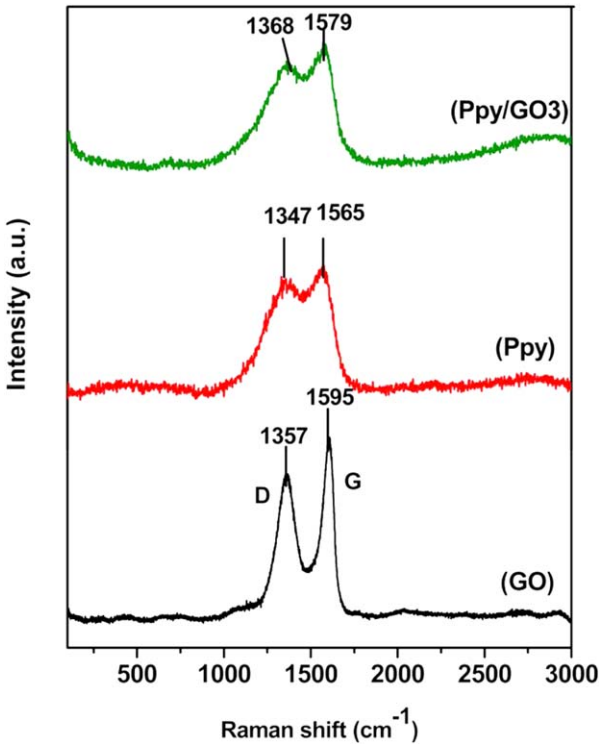

Figure 4. Raman spectra for GO, Ppy, and Ppy/GO3 nanocomposite. [Color figure can be viewed in the online issue, which is available at wileyonlinelibrary.com.]

interlayer distance between GO layers is about 0.737 nm which is larger than that of pristine graphite (0.335 nm), implying the exfoliation of graphite.[31] Pure Ppy, exhibited a weak and broad diffraction peak from 15° to 23°, which indicated the Ppy to be amorphous in nature. For Ppy/GO3 nanocomposite, one broad and high intense peak appeared at around 25.5° which was the characteristic peak of Ppy. Additionally, the characteristic peak of GO within the nanopcomposites disappeared, illustrating the complete coating of Ppy between the layered GO.[32]

Figure 4 shows the Raman spectra for the developed Ppy/GO nanocomposite as well as for pure Ppy and GO layer. Two intense bands at 1357 cm^{-1} and 1595 cm^{-1} for GO have been assigned to D band and G band, respectively. The G band assigned to the first-order scattering of the E_{2g} phonon of GO represents the in-plane bond stretching vibration of sp^2-bonded carbon atoms in a 2D hexagonal lattice. The D band can be associated with the breathing mode of K-point phonons of A_{1g} symmetry with vibration of carbon atoms with dangling bonds in plane terminations of disordered graphite.[33,34] In the Raman spectrum of pure Ppy, the characteristic bands that appeared at 1565 and 1347 cm^{-1} were assigned to the C═C backbone stretching and the ring stretching vibration of Ppy, respectively.[35] In the Raman spectrum of Ppy/GO3 nanocomposite, the D band became broad during the *in situ* polymerization process. In addition, both D and G band shifted to 1368 and 1579 cm^{-1}, when GO was introduced into the Ppy matrix. This was probably due to the doping of carboxyl group of GO to Ppy backbone and π-π interaction between Ppy and GO sheets.[2]

The surface morphologies and shape of the Ppy, GO, and Ppy/GO are shown in Figure 5. The pure Ppy shows an irregular sphere like structure in the order of ~150 to 200 nm. The GO sheets composed of a few layers stacked slackly, whereas morphological structure of the composite varied from the pure materials which could be attributed to the polymerization of Ppy particles on the surface of GO sheets; it was difficult to distinguish the individual phases. The effect of increase in mass ratios of GO in the Ppy/GO nanocomposite (Ppy/GO1, Ppy/GO3, and Ppy/GO5) surface morphology are shown in Figure 6. The images show that all the GO sheets were homogeneously coated with polymer and that the Ppy had mainly grown on the surface or intercalated between the GO sheets. In the case of lower mass ratios of GO added in the nanocomposite, the Ppy particles grown on all GO sheets with larger size when compared with higher mass ratios of GO in the nanocomposite. The higher mass ratios of GO added nanocomposites showed flakey like morphology with Ppy particles intercalated at the edges of GO sheets. The GO sheets were not fully coated by Ppy particles due to the higher amount of GO layers.

The room-temperature electrical conductivity of pure Ppy and Ppy/GO nanocomposites were determined using two probe resistivity measurement system as shown in Figure 7. The *in situ* polymerization of pure Ppy, with HCl as a medium, shows a conductivity of 0.180 S/cm which was lower than that of Ppy synthesized by the electrochemical method (10–50 S/cm)[36] but higher than that of Ppy synthesized by the chemical method using $FeCl_3$ as the oxidant (0.070 S/cm).[37] The room-temperature conductivity of GO film with the thickness of 1 μm was 1×10^{-6} S/cm,[23] which showed insulating property. However, when GO was exfoliated into nanosheets, the π-π electron stacking between the pyrrole ring of Ppy and unoxidized domain of GO could transfer electrons more effectively according to the new conception "GO sheets" proposed by Cho and Lee.[38] The conductivity of Ppy/GO nanocomposite at room temperature reached 0.346 S/cm, which is higher than that of pristine Ppy and GO. The nanocomposite showed an increase of conductivity even at a low GO mass ratio. For Ppy/GO1, Ppy/GO2, Ppy/GO3, Ppy/GO4, and Ppy/GO5, the conductivities were 0.289, 0.297, 0.317, 0.341, and 0.346 S/cm, respectively, at room temperature. The structure of Ppy/GO nanocomposite had improved electrical conductivity probably due to the large surface area of GO sheet that served as a bridge, thereby increasing the conductivity of Ppy/GO nanocomposites.

TGA studies were carried out to study the thermal stability of Ppy, GO, and Ppy/GO nanocomposites as shown in Figure 8. GO sheet first started to lose weight upon heating from 50°C to 150°C because the evaporation of water present between the layers in GO; a second major weight loss occurred at above 300°C which might have been due to the decomposition of oxygen containing functional groups (such as C—OH, C—O—C, COOH) producing CO_2, CO, and H_2O which were removed from the GO nanosheets. For the pure Ppy, the Ppy was stable in the temperature range up to 200°C and showed only about 15% mass loss which could be due to dehydration of the Ppy. However, a rapid weight loss took place after 300°C, which corresponded to the complete degradation and decomposition of

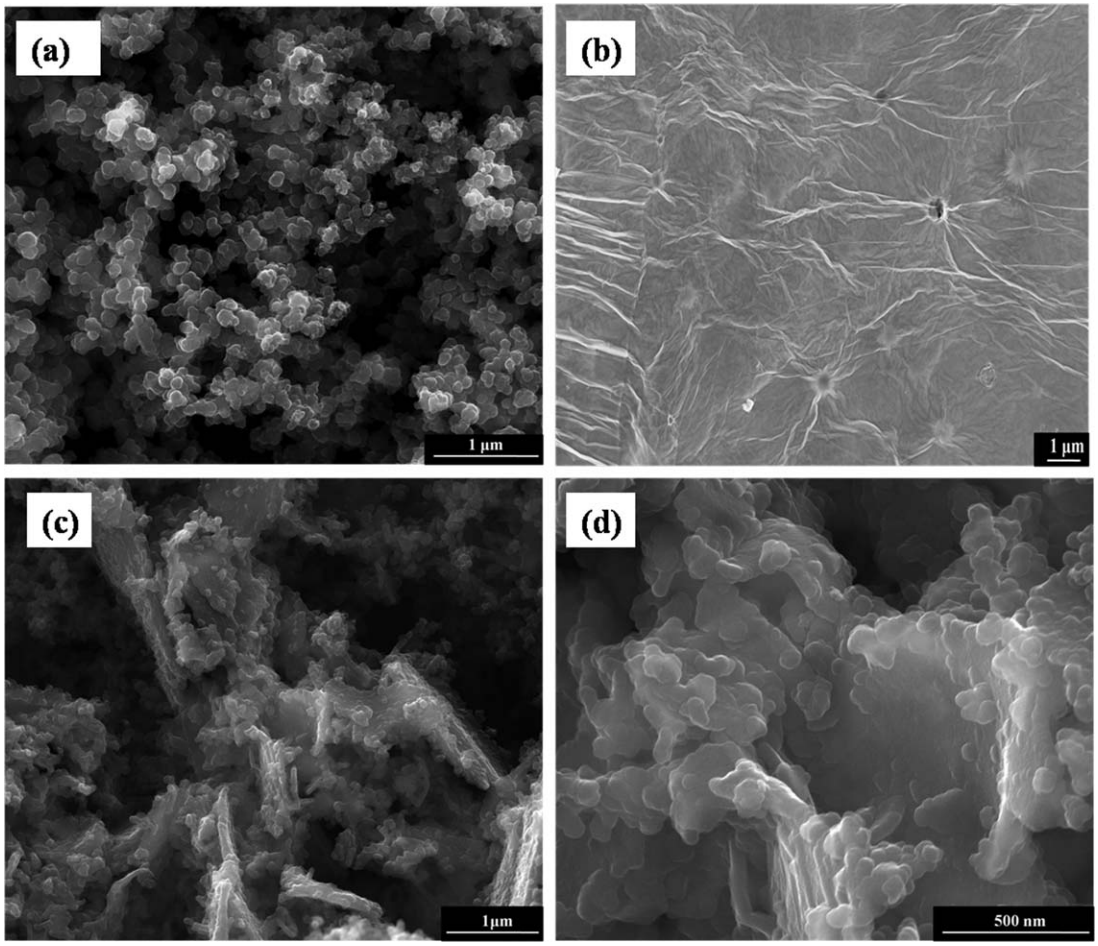

Figure 5. FE-SEM images of (a) Ppy, (b) GO, and (c, d) Ppy/GO3 nanocomposite.

Ppy at different polymerization stage. In Ppy/GO nanocomposite, the slow weight loss up to 200°C can be attributed to the loss of co-intercalated water molecules and pyrolysis of the liable oxygen containing functional groups. After 200°C, major weight loss occurred which might be due to the decomposition of the Ppy. Also, the residual weight loss value of the nanocomposite was found to have increased in comparison with the pure Ppy. The Ppy/GO5 nanocomposite showed nearly 37% weight retention at 700°C which was probably due to the existence of a carbon structure in the nanocomposites.[30]

Rheological Behavior of Ppy/GO Nanocomposite Suspension

Figure 9(A) shows the rheological behavior of pure Ppy and Ppy/GO nanocomposite suspension; they were analyzed by using shear stress as a function of shear rate at 25°C and 150°C. The shear stress exhibited almost linear curve for both pure Ppy and Ppy/GO nanocomposite. The shear stress curve increased linearly with increasing shear rate at 25°C. There was no change in flow behavior of both Ppy and Ppy/GO nanocomposite suspension, but the nanocomposite stress values were high compared with pure Ppy suspension. The sample indicated Non-Newtonian flow behavior, when the temperature was increased to 150°C. The shear stress of pure Ppy suspension increased suddenly in the shear rate ranging from 450 to 1000 S^{-1} at higher temperatures. However, pure Ppy can withstand stress up to 450 S^{-1} at higher temperature. The Ppy/GO nanocomposite suspension also indicated Non-Newtonian flow behavior at low shear rate and Newtonian flow behavior at higher shear rate. Due to the Ppy growth in the pores and galleries of GO sheet surface, the Ppy/GO nanocomposite suspension does not deform at high temperature and at high shear rate. The rheological behavior of Ppy/GO nanocomposite was mainly affected by the following factors on addition of GO. The higher surface area and flexibility of the GO sheet with Ppy particles could have improved the rheological behavior.

Figure 9(B) shows the shear stress flow curve of various mass ratios of GO sheet (1–5%) in the Ppy/GO nanocomposite suspension at 25°C and 150°C. The curve increased linearly with increasing shear rate at 25°C. This was due to the internal strength of Ppy/GO nanocomposite which resisted deformation when the suspension was subjected to shear force. The shear stress values increased with addition of GO sheet in the Ppy/GO nanocomposite and the Non-Newtonian behavior occurred at low shear rate up to 10 γ S^{-1}. In the low shear rate region, where the electrostatic interaction is dominant, the aligned particles begin to break with shear deformation and the broken structures tend to form chains again.[39] The transition from the Non-Newtonian to Newtonian behavior occurred upon increase of shear rate. Ppy/GO nanocomposite exhibited considerable

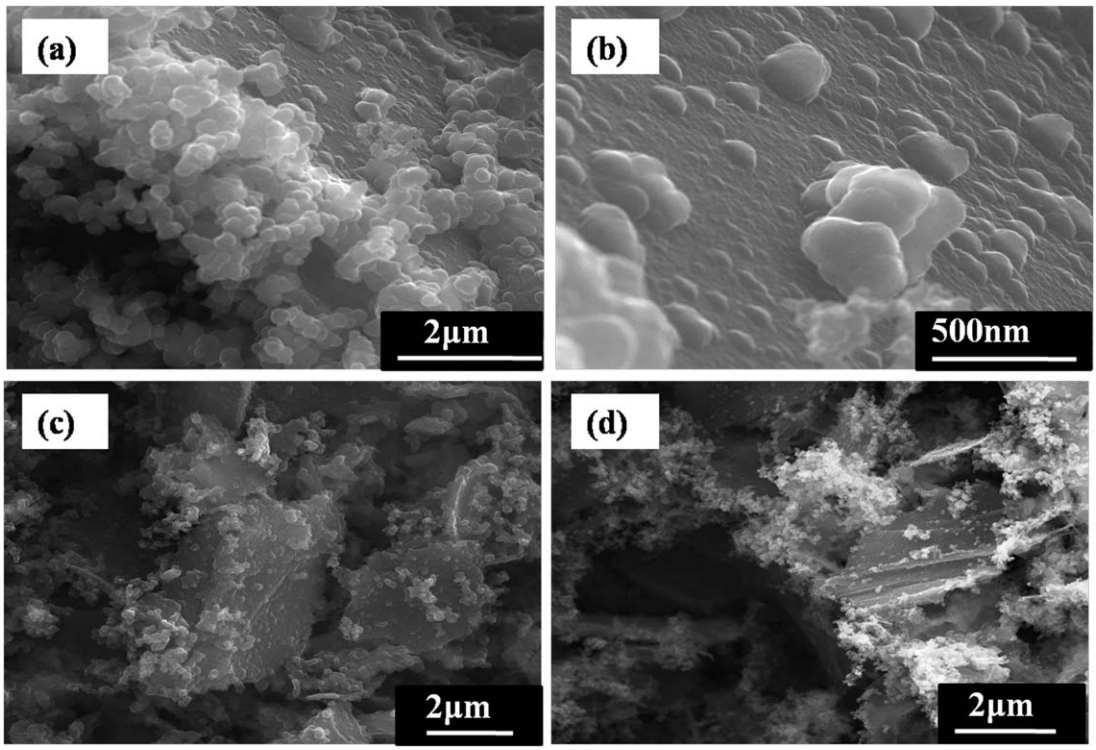

Figure 6. FE-SEM images of GO mass ratio effect in Ppy/GO nanocomposite: (a, b) Ppy/GO1, (c) Ppy/GO3, and (d) Ppy/GO5.

stability in both low and high temperature and showed no deformation even at high shear rate. In addition, in accordance with the FE-SEM observation (Figure 6), the combination of Ppy and GO could be responsible for the rheological properties than the starting component. In this case, rheological properties increased with addition of GO in the nanocomposite. The Ppy particles were grown on all GO sheets at lower mass ratio of GO and the higher mass ratios of GO added nanocomposites showed flake like structure with Ppy particles coated at the edge of GO sheets. The influence of flexible flake like GO sheet could be responsible for increased rheological properties.

The shear stress and linear fit values for pure Ppy and Ppy/GO nanocomposite suspension at 25°C and 150°C have been tabulated in Table I. From the table, pure Ppy stress curve values were exhibited linearly ($R^2 = 0.9999$) and the linearity of Ppy/GO nanocomposite was found to have decreased (Ppy/GO1-$R^2 = 0.9991$, Ppy/GO2-$R^2 = 0.9991$, Ppy/GO3-$R^2 = 0.9967$, Ppy/GO4-$R^2 = 0.9967$, and Ppy/GO5-$R^2 = 0.9818$) in comparison

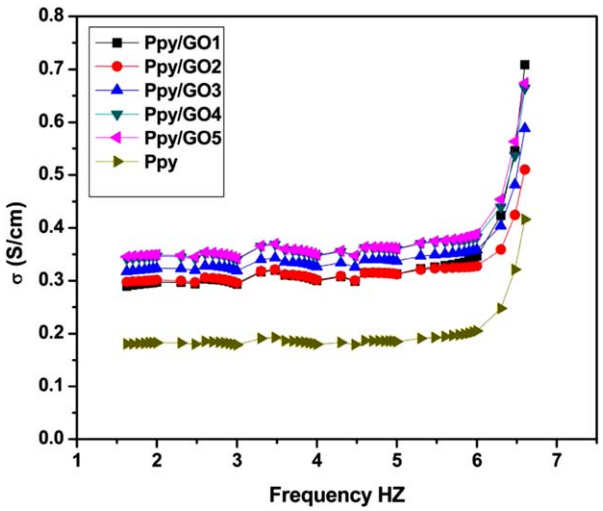

Figure 7. Electrical conductivity for pure Ppy and Ppy/GO nanocomposite. [Color figure can be viewed in the online issue, which is available at wileyonlinelibrary.com.]

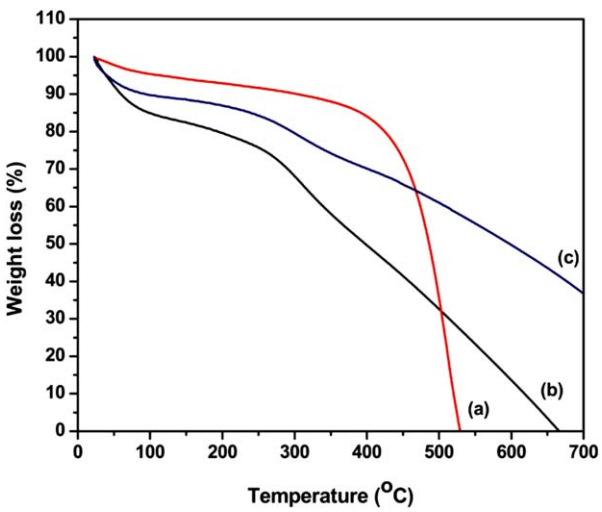

Figure 8. TGA curve of (a) GO, (b) Ppy, and (c) Ppy/GO nanocomposite. [Color figure can be viewed in the online issue, which is available at wileyonlinelibrary.com.]

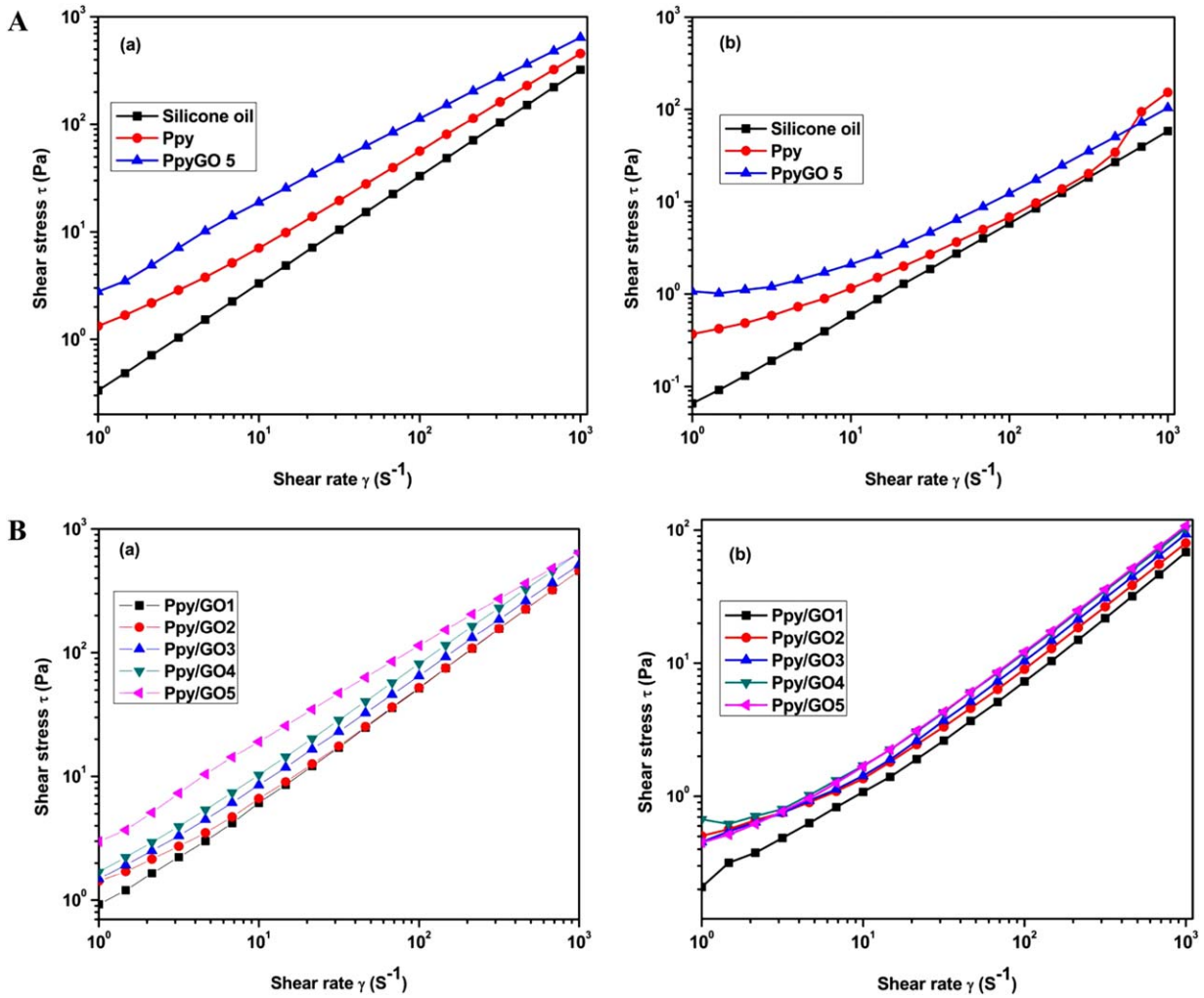

Figure 9. A: The flow curves of shear rate and shear stress of silicone oil, Ppy, and Ppy/GO nanocomposite suspension for (a) 25°C and (b) 150°C. B: The flow curve of shear rate and shear stress of various GO additions in Ppy/GO nanocomposite suspension for (a) 25°C and (b) 150°C. [Color figure can be viewed in the online issue, which is available at wileyonlinelibrary.com.]

with the pure Ppy at 25°C. Furthermore, the linearity of pure Ppy ($R^2 = 0.9334$) decreased when the temperature was increased to 150°C. However, the stress values of Ppy/GO nanocomposite increased in comparison with the pure Ppy at higher temperature. For Ppy/GO1, Ppy/GO2, Ppy/GO3, Ppy/GO4, and Ppy/GO5, the stress values linearity were found to be $R^2 = 0.9999$, $R^2 = 0.9998$, $R^2 = 0.9997$, $R^2 = 0.9997$, and $R^2 = 0.9997$, respectively, at 150°C.

Figure 10(A) shows the typical viscosity obtained for the suspension of Ppy and Ppy/GO nanocomposite in the solution of silicone oil. Graph was plotted between viscosity and shear rate at a constant volume fraction 50 mg/mL for both Ppy and the nanocomposite at 25 and 150°C. There is no significant shear thickening behavior observed at 25°C for both Ppy and Ppy/GO nanocomposite suspension over the wide range of shear rate. The viscosity level of nanocomposite increased when compared

Table I. The Shear Stress and Linear Fit Values of Pure Ppy and Ppy/GO Nanocomposite Suspension at 25°C and 150°C

		1 γ (S^{-1})		10 γ (S^{-1})		100 γ (S^{-1})		1000 γ (S^{-1})		R^2	
S. No	Sample	25°C	150°C	25°C	150°C	25°C	150°C	25°C	150°C	25°C	150°C
1	Pure Ppy	1.32	0.36	7.06	1.15	56.40	6.80	453	152.66	0.9999	0.9334
2	Ppy/GO1	0.92	0.20	6.11	1.08	51.60	7.28	455	68.40	0.9991	0.9999
3	Ppy/GO2	1.42	0.50	6.61	1.36	52.10	9.01	460	80.20	0.9991	0.9998
4	Ppy/GO3	1.49	0.45	8.50	1.43	65.00	10.40	513	93.60	0.9967	0.9997
5	Ppy/GO4	1.69	0.67	10.30	1.70	81.30	11.90	638	103.60	0.9967	0.9997
6	Ppy/GO5	2.98	0.45	19.10	1.68	114.	12.20	642	108.00	0.9818	0.9997

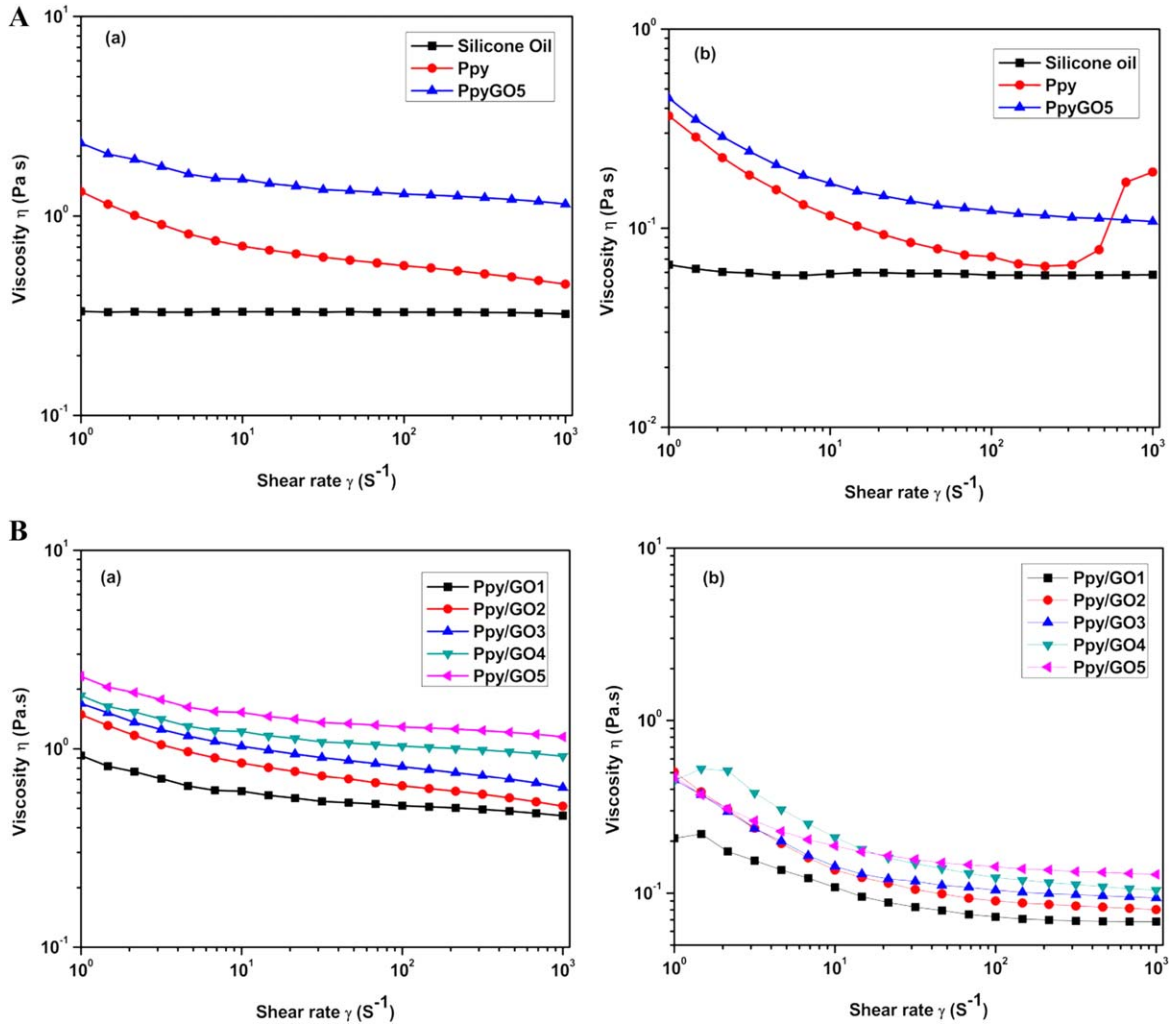

Figure 10. A: The flow curves of shear rate and viscosity of silicone oil, Ppy, and Ppy/GO nanocomposite suspension for (a) 25°C and (b) 150°C. B: The flow curve of shear rate and Viscosity of various GO additions in Ppy/GO nanocomposite suspension for (a) 25°C and (b) 150°C. [Color figure can be viewed in the online issue, which is available at wileyonlinelibrary.com.]

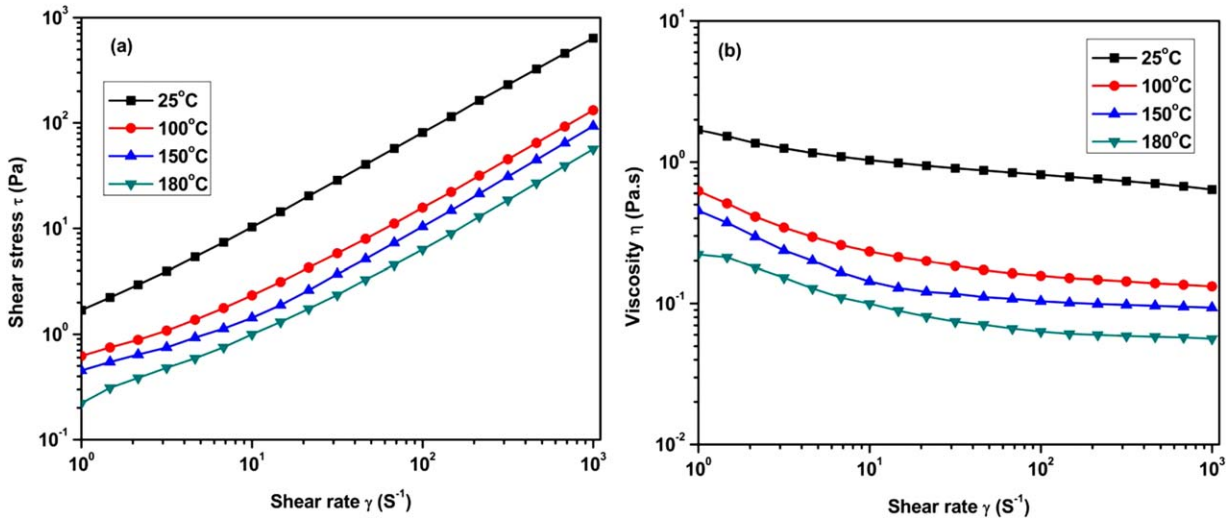

Figure 11. Different temperature effect flow curve of 3% GO addition of Ppy/GO nanocomposite suspension for (a) shear rate vs. shear stress and (b) shear rate vs. viscosity. [Color figure can be viewed in the online issue, which is available at wileyonlinelibrary.com.]

with the pure Ppy. It might have been due to the even dispersion of GO in Ppy which served to increase the viscosity of the suspension. Also, the viscosity measurement for both Ppy and Ppy/GO nanocomposite suspension were carried out at 150°C. The viscosity of pure Ppy gradually decreased and it showed shear thinning behavior up to moderate shear rate. On the other hand, the viscosity suddenly increased and its behavior transition from shear thinning to shear thickening occurred at higher shear rate. Particulate suspensions can show shear thickening behavior if subjected to the right conditions (combination of interparticle forces, particle size, and hydrodynamic interactions). Hydrodynamic interactions become dominant in the high-shear rate region, where particle structures are fully destroyed without reformation, and the suspension behaves like a shear thickening fluid.[38] For the Ppy/GO nanocomposite suspension, the degree of shear thinning increased and the transition from Non-Newtonian to Newtonian flow behavior occurred at high shear rate. The addition of GO sheet to Ppy induced increase in the viscosity to a certain extent. However, the Ppy evenly deposited on the GO sheets would avoid the free Ppy inter particle force in the nanocomposite. The interparticle force and hydrodynamic interactions were removed because of GO sheets in the nanocomposite and contributed to shear thinning behavior.

Figure 10(B) shows the plot between viscosity and shear stresses for various mass ratio of GO added to Ppy at 25 and 150°C. It was observed that the nanocomposites with all the mass ratios chosen showed shear thinning behavior and it was very prominent at low temperature, and the viscosity was increased by the addition of GO sheet in the Ppy which could be due to the GO sheets binding with Ppy by H-bonding and π-π interaction. Therefore, this GO sheet acts as a backbone for the Ppy and it helps for the even dispersion of colloidal solution of nanocomposite and against to the agglomerated polymer particles at high temperature and shear rate.

Figure 11(a,b) shows the rheological behavior of Ppy/GO3 nanocomposite suspension analyzed by shear stress and shear viscosity as a function of shear rate at different temperatures (25, 100, 150, and 180°C). The entire shear stress curve increased with increasing shear rate. The shear stress values were found to decrease by increasing temperature with Non-Newtonian to Newtonian flow behavior. This may be due to the π-π conjugation and hydrogen bond strength of Ppy/GO nanocomposite reduction by high temperature. However, this Ppy/GO nanocomposite showed considerable stability without deformation at 180°C temperature and shear rate. This could be due to the role of GO sheet as a backbone for nanocomposite suspension. From viscosity curve, we observed that the shear thinning behavior increased with increase in temperature.

CONCLUSION

Ppy/GO nanocomposites have been successfully synthesized by *in situ* polymerization. FTIR, XRD, and Raman spectrum revealed the incorporation of GO into the Ppy matrix and the surface morphology was observed by FE-SEM. The electrical conductivity of the nanocomposite increased from 0.289 S/cm to 0.346 S/cm with increase in GO mass ratios added compared with the conductivity of pure Ppy (0.180 S/cm). The Ppy/GO nanocomposite showed improved thermal stability compared to the pure Ppy, in the temperature range 50–700°C. The rheological results showed that the shear stress (τ Pa) and viscosity (η Pa s) of the Ppy/GO nanocomposites was higher than that of the pure Ppy. This result is accompanied by increased flexibility and shear thinning properties of the nanocomposites. We suggest that the developed polymer/inorganic nanocomposite with improved rheological, electrical properties and with higher thermal stability could be the best candidate for industrial applications.

ACKNOWLEDGMENTS

This work was supported by the Council of Scientific and Industrial Research, New Delhi for the award of Senior Research Fellow (SRF) to P. Manivel is gratefully acknowledged.

REFERENCES

1. Kim, H.; Abdala, A. A.; Macosko, C. W. *Macromolecules* **2010**, *43*, 6515.
2. Bora, C.; Dolui, S. K. *Polymer* **2012**, *53*, 923.
3. Muller, D.; Rambo, C. R.; Recouvreux, D. O. S.; Porto, L. M.; Barra, C. M. O. *Synth. Met.* **2011**, *161*, 106.
4. Xing, S.; Zhao, G.; Yuan, Y. *Polym. Compos.* **2008**, *29*, 22.
5. Han, Y.; Lu, Y. *Compos. Sci. Technol.* **2009**, *69*, 1231.
6. Vicentini, D. S.; Barra, G. M. O.; Bertolino, J. R.; Pires, A. T. N. *Eur. Polym. J.* **2007**, *43*, 4565.
7. Gopalan, A. I.; Lee, K. P.; Santhosh, P.; Kim, K. S.; Nho, Y. C. *Compos. Sci. Technol.* **2007**, *67*, 900.
8. Wang, J.; Xu, Y.; Chen, X.; Sun, X. *Compos. Sci. Technol.* **2007**, *67*, 2981.
9. Boukerma, K.; Piquemal, J. Y.; Chehimi, M. M.; Mravcakova, M.; Omastova, M.; Beaunier, P. *Polymer* **2006**, *47*, 569.
10. Novoselov, K. S.; Geim, A. K.; Morozov, S. V.; Jiang, D.; Zhang, Y.; Dubonos, S. V.; Grigorieva, I. V.; Firsov, A. A. *Science* **2004**, *306*, 666.
11. Geim, A. K.; Novoselov, K. S. *Nat. Mater.* **2007**, *6*, 83.
12. Allen, M. J.; Tung, V. C.; Kaner, R. B. *Chem. Rev.* **2009**, *110*, 132.
13. Zhu, C.; Zhai, J.; Wen, D.; Dong, S. *J. Mater. Chem.* **2012**, *22*, 6300.
14. Liu, N.; Luo, F.; Wu, H.; Liu, Y.; Zhang, C.; Chen, J. *Adv. Funct. Mater.* **2008**, *35*, 1518.
15. Cassagneau, T.; Guerin, F.; Fendler, J. H. *Langmuir* **2000**, *16*, 7318.
16. Li, D.; Muller, M. B.; Gilje, S.; Karner, R. B.; Wallance, G. G. *Nat. Nanotechnol.* **2008**, *3*, 101.
17. Zhu, C.; Guo, S.; Fang, Y.; Dong, S. *ACS Nano* **2010**, *4*, 2429.
18. Cassagneau, T.; Fendler, J. H.; Johnson, S. A.; Mallouk, T. E. *Adv. Mater.* **2000**, *12*, 1363.
19. Cassagneau, T.; Fendler, J. H. *J. Phys. Chem. B* **1999**, *103*, 1789.

20. Kovtyukhova, N. T.; Ollivier, P.; Martin, B. R.; Mallouk, T. E.; Chizhik, S. A.; Buzaneva, E. V.; Gorchinskiy, A. D. *Chem. Mater.* **1999**, *11*, 771.
21. Cassagneau, T.; Fendler, J. H. *Adv. Mater.* **1998**, *10*, 877.
22. Kotov, N. A.; Dekany, I.; Fendler, J. H. *Adv. Mater.* **1996**, *8*, 637.
23. Gu, Z.; Li, C.; Wang, G.; Zhang, L.; Li, X.; Wang, W.; Jin, S. *J. Polym. Sci. Part B: Polym. Phys.* **2010**, *48*, 1329.
24. Matsuo, Y.; Tahara, K.; Sugiem, Y. *Carbon* **1997**, *35*, 113.
25. Liu, P. G.; Gong, K. C.; Xiao, P.; Xiao, M. *J. Mater. Chem.* **2000**, *10*, 933.
26. Bissesur, R.; Liu, P. K. Y.; Scully, S. F. *Synth. Met.* **2006**, *156*, 1023.
27. Zhang, K.; Zhang, L. L.; Zhao, X. S.; Wu, J. *Chem. Mater.* **2010**, *22*, 1392.
28. Wu, T. M.; Lin, S. H. *J. Polym. Sci. Part A: Polym. Chem.* **2006**, *44*, 6449.
29. Bose, S.; Kim, N. H.; Kuila, T.; Lau, K. T.; Lee, J. H. *Nanotechnology* **2011**, *22*, 295202.
30. Konwer, S.; Boruah, R.; Dolui, S. K. *J. Electron. Mater.* **2011**, *40*, 2248.
31. Kyotani, T.; Moriyama, H.; Tomita, A. *Carbon* **1997**, *35*, 1185.
32. Xu, J.; Wang, K.; Zu, S. Z.; Han, B. H.; Wei, Z. *ACS Nano* **2010**, *4*, 5019.
33. Manivel, P.; Ramakrishnan, S.; Kothurkar, N. K.; Ponpandian, N.; Mangalaraj, D.; Viswanathan, C. *J. Exp. Nanosci.* **2013**, *8*, 311.
34. Liu, Y.; Deng, R.; Wang, Z.; Liu, H. *J. Mater. Chem.* **2012**, *22*, 13619.
35. Wang, J.; Xu, Y.; Zhu, J.; Ren, P. *J. Power Sources* **2012**, *208*, 138.
36. Deepa, M.; Ahmed, S. *Eur. Polym. J.* **2008**, *44*, 3288.
37. Wang, C. G.; Yang, Z.; Li, X.; Li, C. Z. *Carbon* **2005**, *43*, 2564.
38. Cho, S. I.; Lee, S. B. *Acc. Chem. Res.* **2008**, *41*, 699.
39. Zhang, W. L.; Choi, H. J. *Langmuir* **2012**, *28*, 7055.